Photochemical & Photobiological Sciences

Gas-phase energy of the S2←S0 transition and electrostatic properties of the S2 state of carotenoid peridinin via solvatochromic shift and orientation broadening of absorption spectrum

Journal:	*Photochemical & Photobiological Sciences*
Manuscript ID:	PP-ART-04-2014-000124.R1
Article Type:	Paper
Date Submitted by the Author:	13-Jun-2014
Complete List of Authors:	Pavlovich, Vladimir; Military Academy of Belarus, Division of higher mathematics and physics

Gas-phase energy of the $S_2 \leftarrow S_0$ transition and electrostatic properties of the S_2 state of carotenoid peridinin via solvatochromic shift and orientation broadening of absorption spectrum

Vladimir S. Pavlovich

Division of higher mathematics and physics
Military Academy of Belarus
Prospect Nezalejnaszy 220, Minsk 220057, Belarus
E-mail: u.s.paulovich@tut.by

The solvent effect on the position and the shape of absorption spectrum of peridinin for 12 protic and aprotic solvents as well as the temperature effect for methanol were studied using a solvatochromic theory based on the Onsager sphere-cavity model. (Experimental data have been provided by T. Polivka and V. Sundström.) Solvatochromic calculations combined with estimations of orientation broadening of absorption spectrum by convolution allowed to conclude that the orientation (dipole-dipole), induction and dispersion solute-solvent interactions describe reasonably the position of the 0-0 frequency. The orientation interactions led to the blue solvatochromic shift, separating them from the induced and dispersion interactions, which produce red shift. The FWHM of Gaussian of inhomogeneous broadening originated from the fluctuations of orientation interactions is demonstrated to be high of 945 cm^{-1} even for such nonpolar solvent as hexane. The value $|\mathbf{\Delta\mu}|/\cos\varphi$ of -18.7 D has been found ($\mathbf{\Delta\mu}=\mathbf{\mu}_2-\mathbf{\mu}_g$, φ is the angle between $\mathbf{\Delta\mu}$ and $\mathbf{\mu}_g$). By assigning peridinin to the idealized C_{2v} point group, the large change of dipole moment $|\mathbf{\Delta\mu}|$ of 18.7 D under $S_2 \leftarrow S_0$ transition is obtained for peridinin in gas phase (for the solute free from environment). Moreover, the S_2 excited-state dipole moment $\mathbf{\mu}_2$ has the opposite orientation relative to that at the ground S_0 state $\mathbf{\mu}_g$. The determined gas-phase 0-0 energy of the $S_2 \leftarrow S_0$ transition of 22910 cm^{-1} (2.84 eV) is employed to calculate the polarizability change between the S_0 and S_2 states of 376 $Å^3$. The finding for the effective Onsager radius is of 9.4 Å. Obtained results for electrostatic properties of S_2 state are compared with those known from Stark spectroscopy and quantum-mechanical calculations.

Introduction

Carotenoids serve a number of vitally important functions in various organisms. In photosynthesis, they act as light harvesters, as regulators of energy flows, as photoprotectors and antioxidants to prevent the generation of high-reactive singlet oxygen.[1-7] The protective effect is achieved not only through the rapid quenching of chlorophyll triplets, but also through direct deactivation of singlet oxygen. These unique functional abilities of carotenoids directly relate to their molecular structure resulting in atypical order of electronic levels. It is commonly assumed that carotenoids, similar to polyenes, belong to the idealized C_{2h} point group. The lowest excited state $2A_g^-$ is then forbidden for one-photon processes, because it carries gerade symmetry of the ground state $1A_g^-$. The strong absorption in the visible region

is due to allowed transition between the $1A_g^-$ state and the second excited state $1B_u^+$.[8,9] Existence of other optically forbidden states ($1B_u^-$ and/or $3A_g^-$) between the $2A_g^-$ and $1B_u^+$ states predicted theoretically for polyenes with six or more conjugated doubles bonds[10], has been observed for some carotenoids in experiments.[11,12] Yet, for the carotenoid in this study, peridinin, both these states lies above the absorbing $1B_u^+$ state.[13] Therefore, we will employ here the generally-used notation S_0, S_1, S_2 to denote the $1A_g^-$, $2A_g^-$, $1B_u^+$ states.

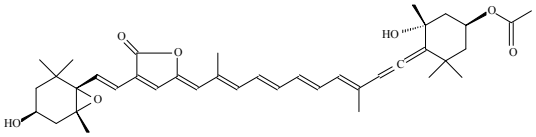

Scheme 1. Molecular structure of peridinin.

Peridinin (Scheme 1) is the principle carotenoid of the light harvesting complexes in dinoflagellates.[14,15] In the water-soluble peridinin-chlorophyll protein (PCP), peridinin even serves as a major light-harvesting pigment. It belongs to the family of carbonyl carotenoids whose conjugated carbonyl group alters significantly the excited-state properties by introducing an intramolecular charge transfer (ICT) state into the excited-state manifold.[16,17] The typical effect attributed to the presence of the ICT state is polarity-dependent lifetime of the lowest excited state. It has been shown that the lifetime of peridinin varies from 7 ps in highly polar solvents to 170 ps in the nonpolar solvents.[16-19] The strong polarity dependence of lifetime peculiars also to uriolide acetate, fucoxanthin[17] and especially to apocarotenals.[20-22] Besides the polarity-dependent lifetime, energies and spectral profiles of the absorption and emission bands as well as the quantum yield of fluorescence are also highly affected by solvent environment.[16-23]

In peridinin, the effects of the conjugated carbonyl group are among the strongest observed so far, which may be attributed to the location of the conjugated carbonyl group at a lactone ring and presence of the allene group in the π-electron conjugation. Molecular orbital calculations[13,24] suggested electron-charge density redistribution from the allene to the lactone upon the $S_2 \leftarrow S_0$ transition. Using the MNDO-PSDCI calculations Shima et al. [13] concluded that the change of permanent dipole moment (DM) between S_1 and S_0 state comprises of 7.49 D. Their finding for DM at S_1 state by analysis of solvatochromic shift of absorption and fluorescence spectra was about 16 D in both polar and nonpolar environments with calculated DM at S_0 state of 5.97 D. In contrast to the MNDO-PSDCI calculation yielding change of DM for $S_2 \leftarrow S_0$ transition $\Delta\mu$ of 2.2 D[13] significantly larger value of 22 and ~27 D, at 77 K for peridinin in methyl tetrahydrofuran and ethylene glycol respectively, was found by Stark spectroscopy.[25] Premvardhan et al.[25] are noted that this results are supported by solvatochromic calculations when an ellipse-cavity model is employed. The large values of $\Delta\mu$ upon $S_2 \leftarrow S_0$ transition

were also obtained for another carbonyl carotenoid fucoxanthin.[26] The negative Δμ of -6.18 D was recently obtained by Wagner et al.[27] using the SAC-CI calculations for a peridinin model compound in methanol.

The change of DMs during absorption, radiative and nonradiative transitions between electronic states is closely allied to the ICT dynamics.[13,16-32] However at the moment there is no clear consensus on both the CT nature of the excited states and on their DMs for peridinin. It should be also mentioned that there are a few reports[13,24,25] dealing with calculations of peridinin intermolecular interactions in solutions. Onsager dipole-in-a-sphere model is used to estimate the dipole-dipole (orientation) solvation energy at the ground and excited states.[24] Apart from analytical spectral-shift calculations for a number solvents[25] the semiempirical calculations of level ordering were carried out for peridinin-water clusters[13] as well as for six solvents[27] in very simplified solvent-environment model. The large values of Δμ for the $S_2 \leftarrow S_0$ transition obtained by Stark spectroscopy, both for peridinin[25] and related fucoxanthin,[26] also added to a rebirth of interest in solvatochromic shift of peridinin absorption.

In this paper we show that the environment effect on the absorption spectrum can be adequately described by classical theory of intermolecular interactions through the application of the continuum Onsager model.[33] The calculations provide the direct determination of DM and polarizability changes as well as the gas-phase 0-0 frequency for the $S_2 \leftarrow S_0$ transition. We argue that Δμ upon transition between S_0 and S_2 states of 18.7 D is negative, and that the DMs at the S_0 and S_2 states have opposite direction.

Theoretical backgrounds and results and discussion

1. Solvatochromic shift

Solvatochromic shift has its origin in the changes of both DM and polarizability of the solute upon absorption of light, provoking differential solvation energy of the ground and excited electronic states. We will ignore influence of repulsive interactions and H-bonding and write solvent dependent shift of the maximum position (or the 0-0 transition energy) of absorption spectrum as follows

$$\Delta\nu = \Delta\nu_{or} + \Delta\nu_{ind} + \Delta\nu_{dis} =$$

$$= -\frac{2\boldsymbol{\mu}_g(\boldsymbol{\mu}_e - \boldsymbol{\mu}_g)}{a_O^3}\frac{\varepsilon - 1}{2\varepsilon + 1} - \frac{(\boldsymbol{\mu}_e - \boldsymbol{\mu}_g)^2}{a_O^3}\frac{n^2 - 1}{2n^2 + 1} - \frac{3\Delta\alpha_{eg}}{a_O^3}\frac{E_{00}^2 I_s}{I_s^2 - E_{00}^2}\frac{n^2 - 1}{n^2 + 2}. \quad (1)$$

In eq. (1) the first two terms $\Delta\nu_{or}$ and $\Delta\nu_{ind}$ represent the solvatochromic shifts due to orientation and induction interactions adopted in accordance with Ooshika-Lippert-Mataga-McRae theory.[34-40] The last term $\Delta\nu_{dis}$ represents a component of the shift due to dispersion interactions via formula derived in Ref [41]. The $\boldsymbol{\mu}_e$, $\boldsymbol{\mu}_g$, α_e, α_g are the gas-phase DMs and polarizabilities of excited (*e*) and ground (*g*) states of

the solute molecule, respectively; $\Delta\alpha_{eg}=\alpha_e-\alpha_g$; and E_{00} is the energy gap between *e* and *g* states for free (gas-phase) solute molecule; I_s is the ionization potential of solvent molecule; ε and *n* are dielectric constant and refractive index of the solvent. In the Onsager model[33] a probe dipole is placed at the center of a spherical cavity. Therefore here the Onsager radius of the solute a_O is an effective value, because for such linear molecule as peridinin the assumption of spherical shape of cavity is far apart from reality.

The following quantities will be used for convenience

$$P_\varepsilon = \frac{\varepsilon - 1}{2\varepsilon + 1},\ \Pi_n = \frac{n^2 - 1}{2n^2 + 1},\ P_n = \frac{n^2 - 1}{n^2 + 2},$$

where P_ε represents the bulk solvent polarity; Π_n and P_n represent two kinds of the bulk polarizability of solvent based on Onsager and Clausius-Mosotti treatment, respectively. There are three key unknowns in eq. (1):

$$C_x = C_{or} = -\frac{2\boldsymbol{\mu}_g\left(\boldsymbol{\mu}_e - \boldsymbol{\mu}_g\right)}{a_O^3}, \tag{2}$$

$$C_y = C_{ind} = -\frac{\left(\boldsymbol{\mu}_e - \boldsymbol{\mu}_g\right)^2}{a_O^3}, \tag{3}$$

$$C_z = C_{dis} = -\frac{3E_{00}^2 I_s}{I_s^2 - E_{00}^2}\frac{\Delta\alpha_{eg}}{a_O^3}. \tag{4}$$

Using eqs. (1)-(4) the maximum (or 0-0 transition energy) of absorption spectrum may be given as

$$\nu = \nu_0 + \Delta\nu = \nu_0 + C_x P_\varepsilon + C_y \Pi_n + C_z P_n, \tag{5}$$

where ν_0 is a frequency absorption maximum (or 0-0 transition energy) in gas phase.

Dependence of absorption maximum on solvent polarizability P_n is plotted in fig. 1. As clear the good linear correlations of ν_{max} versus P_n are obtained separately for polar and nonpolar solvents. By this is meant that P_n linearly depends on P_ε and Π_n for these groups of solvents. Nevertheless, just here it should be noted that there is no escape from the conclusion that DM at the S_2 excited state of peridinin is distinct for nonpolar and polar media. Really, as is shown in fig. 1 (inset) the intersection point of regression line with ordinate ν_{max} is 1350 cm^{-1} above for nonpolar solvents then that for polar ones. This difference of 1350 cm^{-1} is in complete agreement with the frequency of peridinin vibration being active in the optical transition.[18] The reason is that for the high polar solvents, in contrast to nonpolar ones, the maximum of spectrum relates to the 0-0 transition. Consequently, in solvatochromic calculations it is necessary to employ the maxima of 0-0 bands ν_{00} for all solvents which are presented as a function of P_n in fig. 2. Such plotting leads to minor intersection difference of 35 cm^{-1}.

The absorption maximum ν_{max} and position of 0-0 transition ν_{00} of peridinin, along with the solvent parameters P_n, P_ε, Π_n, are listed in Table 1. After going from experimental λ to ν, when plotting, we have applied data ν_{max} and ν_{00} without rounding to preclude additional uncertainty under regression.

The standard deviation for ν_{max} and ν_{00} does not exceed 25 cm^{-1}. To estimate P_n, P_ε and Π_n the data for ε and *n* are were taken from handbooks[42-44]. Next notations are used for solvents: *n*-hexane (Hex), *n*-heptane (Hept), benzene (Benz), carbon disulfide (CS2), diethylether (DEE), tetrahydrofuran (THF), 2-propanol (2Prop), methanol (MetOH), acetonitrile (ACN), ethylene glycol (EG), glycerol (Glyc), dimethyl sulfoxide (DMSO).

2. Orientation inhomogeneous broadening. Calculation of C_x, C_y, and C_z

To find the three unknowns C_x, C_y and C_z it is necessary to examine the broadening of absorption spectra resorting to convolution procedure. It is common knowledge[45,46] that the fluctuations of orientation (dipole-dipole) solute-solvent interactions lead to inhomogeneous broadening of spectrum. Taking in attention eq. 3 the relation for the variance of maximum (or 0-0 transition energy) D^2 produced by orientation fluctuations can be expressed[46-49] as

$$D^2 = \frac{2\mathbf{\Delta\mu}^2}{a_O^3} k_B T \frac{\varepsilon - 1}{2\varepsilon + 1} = -2C_y k_B T P_\varepsilon , \qquad (6)$$

where $\mathbf{\Delta\mu}=\mathbf{\mu}_e-\mathbf{\mu}_g$, k_B is Boltzman constant, and T is temperature. Notice, that the eq. (6) is in agreement with earlier general conclusion from Marcus[50] that D^2 varies proportionally to T. Thus, the shape of observed spectrum $\kappa(\nu)$ is a convolution[46,51,52]

$$\kappa(\nu) = \int_0^\infty d\omega \kappa_0(\nu,\omega) G(\omega - \omega_0) \qquad (7)$$

between an individual absorber spectrum $\kappa_0(\nu,\omega)$ with maximum 0-0 band ω and the Gaussian inhomogeneous broadening

$$G(\omega - \omega_0) = \frac{1}{\sqrt{2\pi}D} \exp\left[-\frac{(\omega - \omega_0)^2}{2D^2} \right]$$

with D^2 determined by eq. (6). The full width at half maximum (FWHM) of this Gaussian distribution is the inhomogeneous width of 0-0 band $\Gamma = 2\sqrt{2\ln 2}D$, and ω_0 is a mean of ω. It is noteworthy that $\kappa_0(\nu,\omega)$ is a function of both ν and ω simultaneously. To simplify calculations one considers a simplest case when the individual absorber has unchanged shape of spectrum for any one of ω. The homogeneous broadening is always low and can be neglected. Since for the independent chance events the variances are summed additively[53], and having no any information about individual spectrum $\kappa_0(\nu,\omega)$, we employed spectrum for Hex (fig. 3, inset) in place of $\kappa_0(\nu,\omega)$ to find the relative variance Δ^2 ($\Delta^2 = D^2_{solv} - D^2_{Hex}$) between Hex and any other solvent. To estimate C_y and D^2_{Hex} one write, on eq. (6), that

$$\Delta^2 = -2C_y k_B T P_\varepsilon - D^2_{Hex} . \qquad (8)$$

Following to convolution (7) the calculated spectra $\kappa(\nu)$ are fitted to those observed experimentally $\kappa_{exp}(\nu)$ for diferent solvents. The Δ^2 have been determined when the spectra $\kappa(\nu)$ and $\kappa_{exp}(\nu)$ were equal in the total FWHM. The Δ^2 obtained by such way depends on solvent polarity P_ε as shown in fig. 3. The numerical data for Δ^2 are listed in Table 2 along with D^2 and Γ at 293 K (as well for methanol at 190 K). Some examples of comparison of experimental and calculated spectra are shown in fig. 4.

One may see in fig. 3 that the relative variance Δ^2 as a function of P_ε gives results conforming to linear dependence (8) for nonpolar solvents Hex, Hept, Benz and CS2 as well as for low polar solvents such as DEE and 2PrOH. The linear regression demonstrate the slope of 789110 cm^{-2} with high correlation coefficient r=0.9934. Thus, we have concluded that for this group of solvents the relative broadening is mainly caused by the fluctuations of orientation interactions. Although the quite good liner correlation is observed, it does not include zero point, but this condition has to fulfill for the plot of Δ^2 versus P_ε because $\Delta^2 = D^2 - D^2_{\text{Hex}}$. On the other hand, the minor deviations between experimental $\kappa_{exp}(\nu)$ and calculated $\kappa(\nu)$ spectra are observed for CS2 (fig. 4). Consequently, the broadening of peridinin spectrum is described the best by eqs. (6) and (7) for CS2. On this basis we have employed the slope of 866160 cm^{-2} for solid line connecting two points, Hex and CS2 (fig. 3) to found by eq. (8) C_y=-866160/2k_BT =-2126 cm^{-1}. Such way for handling data has outstripped all expectations. For Hex (Table 2), the variance D^2 of 161132 cm^{-2} calculated by the second part of eq. (6) is in the excellent agreement with parameters of two-points line 866160P_ε-161106 where the value of 161106 cm^{-2} is D^2_{Hex}. Since $\Gamma_{\text{Hex}} = 2\sqrt{2\ln 2}D_{\text{Hex}}$ it immediately follows that the strong Gaussian inhomogeneous broadening with FWHM of 945 cm^{-1} is generated by fluctuations of orientation interactions even for nonpolar Hex. Since for piridinin the S_2 lifetime remains a mystery one employs that of 50 fs known for the allied carotenoid fucoxanthin[54] to estimate the homogeneous width by the relation[55] $\Gamma_{\text{homo}} \approx (2\pi T_1)^{-1}$ (T_1 is the population decay time, the excited state lifetime). We obtain Γ_{homo}≈100 cm^{-1} that is nearly one order of magnitude below then inhomogeneous broadening for Hex. Consequently, the homogeneous broadening can be ignored for all solvents under consideration. What's more because the variance Δ^2 was found as the relative value to Hex, our calculations assure a compensation of the component Γ_{homo} despite the fact that the spectral line shape is Lorentzian.

The large deviations from eq. (6) in behavior of Δ^2 are observed for highly polar solvents, MetOH, ACN, DMSO, EG, and for THF (fig. 3). The possible origins of deviations will be discussed below (section 8). Here one called also attention to other essential features. Whereas good fits of $\kappa(\nu)$ to $\kappa_{exp}(\nu)$ is realized for nonpolar solvents (Hex, Hept, CS2 and Benz), a characteristic feature of peridinin absorption spectrum in THF, 2Prop, MetOH, ACN, DMSO, EG and Glyc, is a superiority of the 0-0 transition intensity in the experimental spectrum $\kappa_{exp}(\nu)$ over that in spectrum $\kappa(\nu)$ calculated by

convolution (7) (fig. 4). This result suggests that individual absorber spectrum $\kappa_0(\nu,\omega)$ is still changed noticeably with variation of maximum 0-0 band ω (section 9).

To obtain the values C_x one takes into account that two kinds of the bulk polarisabilities P_n and Π_n of Hex and 2Prop are practically equal, namely, 0.229 and 0.230 as well as 0.186 and 0.187 respectively. Inasmuch as dispersion and induced components of solvatochromic shift are equivalent for these two solvents, it is evident from eqs. (1) and (5) that $C_x=[\nu_{00(2Prop)}-\nu_{00(Hex)}]/[P_{\varepsilon(2Prop)}-P_{\varepsilon(Hex)}]=1358$ cm^{-1}. Under calculation the experimental $\nu_{00(Hex)}$ of 20618.5 cm^{-1} is used, while for 2Prop the $\nu_{00(2Prop)}$ of 20990.5 cm^{-1} have been estimated as $22864-8145.7P_{n(2Prop)}$ to achieve better accuracy (see captions to figs. 1, 2).

In the case of Hex, Hept and CS2 the good linear regression takes place with the slope of -9636 cm^{-1} and very high r of -0.9999 (fig. 2) for experimental data ν_{00} versus P_n. As is obvious from eq. (5), it is possible only when P_ε and Π_n are linearly dependent on P_n. It should be particularly emphasized that there are two groups of points which include nonpolar solvents, Hex, Hept, Benz, CS2 (fig. 5), and polar ones, MetOH, ACN, 2Prop, EG, DMSO, Glyc. In either group, more or less, P_ε and Π_n are linearly dependent on P_n, therewith for the latter group P_ε remains practically constant. DEE and THF take up intermediate position between these groups, and they are ignored under regression. We eliminated from consideration ν_{00} of Benz, which drops out from the first group unlike its position ν_{max} in fig. 1. The minor cross-point difference of 35 cm^{-1} for two groups of solvents (fig. 2) demonstrates the bright physical result, namely, when $P_n=0$ the peridinin molecules can be treated as though they are in gas phase, and ν_{00} must be alike. The linear plots P_ε versus P_n as well as Π_n versus P_n with nearly equal slope of 0.595 (r of 0.9991 and 0.9999 respectively) are exhibited in fig. 5 for Hex, Hept and CS2. Using these data the numerical estimation for the unknown C_z of -9179 cm^{-1} has been produced, on eq. (5), by the relation $C_z=-9636-0.595(C_x+C_y)$. Differently, we chose Hex, Hept and CS2 as a base for calculation of C_z to use linear properties of eq. (5) under given C_x and C_y. There is no need to discuss on what reason P_ε and Π_n linearly depend on P_n for these solvents because we solve pure mathematical task.

3. Gas-phase 0-0 electronic energy of the $S_2 \leftarrow S_0$ transition

Full solvatochromic shift $\Delta\nu$ as well as its dispersion $\Delta\nu_{dis}$, orientation $\Delta\nu_{or}$ and induction $\Delta\nu_{ind}$ components are calculated according to eqs. (1), (5), when C_x, C_y, C_z equal 1358, -2126, -9179 cm^{-1} respectively. The findings are summarized in Table 1. It was desirable, where possible, to avoid errors, because of this the gas-phase 0-0 absorption maximum of 22910 ($\pm$40) cm^{-1} was determined by plotting $\Delta\nu$ versus ν_{00} only for three base solvents, Hex, Hept and CS2. To account for such choosing, recall that peridinin spectrum for these solvents possesses well-resolved vibration structure (figs. 3, 4) that enables

to determine ν_{00} with acceptable accuracy and, thus, to preclude unnecessarily uncertainty for ν_{00} due to overlapping of 0-0 band with 0-1 one. Since the vibration bands in absorption spectrum of peridinin in solutions are separated by ~1350 cm^{-1}, it is reasonable to assume that the 0-1 transition has the gas-phase energy about 24260 cm^{-1}. Fig. 6 provides the comparison of calculated 0-0 transitions ν_{calc} with experimental data ν_{00} and demonstrates the linear regression with slope of 1.0021 that, ideally, should be of 1.

5. Electric dipole moment at S_2 excited state. Effective Onsager radius

In view of lactone ring the polyene part of peridinin belongs to the C_s point group, therefore the eqs. (2), (3) allow to determine only the value $|\mathbf{\Delta\mu}|/\cos\varphi = 2\mu_g C_y / C_x$ ($|\mathbf{\Delta\mu}| = |\mathbf{\mu}_2 - \mathbf{\mu}_g|$), because we know northing about φ, which may be an arbitrary value in the range from 0 to 180°. Nevertheless, the positive C_x in eq. (2) is possible only when the angle φ between $\mathbf{\mu}_g$ and $\mathbf{\Delta\mu} = \mathbf{\mu}_2 - \mathbf{\mu}_g$ is greater then 90°. By using the ground-state DM of 5.97 D from Shima et al.[13], C_x=1358 cm^{-1} and C_y=-2126 cm^{-1}, one can obtain, that $|\mathbf{\Delta\mu}|/\cos\varphi$=-18.69 D.

As reported by Premvardhan et al.,[25] the Stark spectroscopy measurements of peridinin in methyl THF yield, without the sign, the cosine of the angle between $\mathbf{\Delta\mu}$ and the direction of the $S_2 \leftarrow S_0$ transition dipole moment **m** of 0.98. Consequently, to evaluate the DM in the S_2 state we can, at least for the $S_2 \leftarrow S_0$ transition, relate the molecular structure of peridinin to the idealized C_{2v} point group. The positive C_x in this point group is possible only when φ=180°. With this assumption one can find that the change of DM between S_2 and S_0 states, the component of $\mathbf{\Delta\mu}$ in direction of $\mathbf{\mu}_g$, is given as $\Delta\mu = 2\mu_g C_y / C_x$ to estimate Δμ of -18.7 D. Thus the gas-phase excited-state DM $\mathbf{\mu}_2$ of 12.72 D is *opposite* to that of the ground state $\mathbf{\mu}_g$. As indicated in fig. 6, there is no evidence that $\mathbf{\mu}_2$ depends on solvent polarity because no essential deviations from the liner regression for all points (the slope is of 1.0708, *r*=0.9862). We have drawn the conclusion that $\mathbf{\mu_2}$ is the same both in aprotic and protic solvents.

Our finding of 12.72 D for $\mathbf{\mu}_2$ differs noticeably from that of 18 D from Premvardhan et al.[25] deduced from Stark spectroscopy result of 22 D by correction on a cavity field enhancement. The value Δμ of -18.7 D is far from that of -6.18 D presented by Wagner et al.[27] One further comment is in order that the SAC-CI calculations[27] predict only negative Δμ other then the opposite direction of $\mathbf{\mu}_2$. (The remark in the Supporting material[27] "The dipole moments … in the case of the second and third excited singlet state are in roughly the opposite direction of the ground state dipole moment" is inconsistent with the numerical data, Δμ=-6.18 D and μ_g=8.67 D, presented in main part of paper in fig. 8, because $|\Delta\mu|$ is to be over μ_g.

As follows from eq. (3)

$$a_O^3 = -\Delta\mu^2 / C_y$$

that has enabled the effective Onsager radius a_O of 9.4 Å to be determined. For comparison, one points out the long semi-axis of 13 Å employed in ellipsoid-cavity model.[25] Very low value of 4.5-5 Å[29] was based on the wrong assumption that the solvent effect is originated mainly from lactone ring and partially from polyene chain, while other parts of peridinin molecule are untapped.

6. Change of polarizability upon the $S_2 \leftarrow S_0$ transition

Since peridinin molecule is high anisotropic one, the polarizabilities α_g and α_e are the mean values determined as $\alpha = Tr\boldsymbol{\alpha}/3$, where $\boldsymbol{\alpha}$ is a polarizability tensor of the second order. We embarked on an effort to evaluate the $\Delta\alpha_{eg}$ by eq. (4)[41] employing relation

$$\Delta\alpha_{eg} = -C_z \frac{I_s^2 - E_{00}^2}{3 I_s E_{00}^2} a_O^3 . \qquad (9)$$

The solvent ionization potential I_s is ranged from 9.25 (Benz) to 12.20 eV (ACN).[42] When I_s of 10.4 eV taken as a mean for all solvents, $\nu_{0\text{-}0}$=2.84 eV, C_z=-9179 cm^{-1} and a_O=9.4 $Å^3$, one finds $\Delta\alpha_{eg}$ of 376 $Å^3$. With α_g=127 $Å^3$ obtained for π- and σ-electrons[13] the mean polarizability α_e is of 503 $Å^3$. Krawczyk and Olszowka[56] have found by Stark spectroscopy measurements that $\Delta\alpha$ ranged between 700-1600 $Å^3$ for various carotenoids without lactone ring. Our value of 376 $Å^3$ is lower due to the greater difference in molecular structure of compared carotenoids, since the high polar lactone ring causes a redistribution of the negative charge in polyene chain of peridinin. Such interpretation is supported by the Le Fevre rule[57] that polarizability is markedly reduced whenever the π-electron conjugation system develops strong polarity. Thus, our result $\Delta\alpha_{eg}$=376 $Å^3$ is foolproof, though it is still larger than that of 179 $Å^3$ calculated by the MNDO-PSDCI method.[13]

7. Solvatochromism of peridinin

Solute-solvent coupling effects can be divided into non specific, or universal interactions and specific, or short-range interactions.[58] The bulk influence of solvent as continuous media depends on dielectric constant ε and refractive index *n* of solvent, and thus manifests itself as universal interaction. Since the parameters C_y, C_z are negative, the induced and dispersion universal interactions give rises to the red (bathochromic) shift whereas the orientation interactions cause blue (hypsochromic) shift, because the C_x is positive. It is now possible to answer on the raised question whether the intermolecular repulsive interactions and H-bonding effect are negligibly small and can be ignored in solvatochromic shift for $S_2 \leftarrow S_0$ absorption. In all alcohols under consideration, regardless of their nature and structure, peridinin demonstrates solvatochromic shift for the most part from universal interactions because only minor

deviations are observed from the base line ν_{calc} versus ν_{00} plotted for Hex, Hept and CS2 as well as from that for all solvents (fig. 6). This makes it possible to conclude that in protic media the specific interactions via H-bonding do not affect the position of the 0-0 transition.

Short-range repulsive interactions produce blue (hypsochromic) shift, but there is less information for organic compounds. The most extensively studies of repulsive solvent shift presented for $a^1\Delta_g \rightarrow X^3\Sigma_g^-$ phosphorescence of molecular oxygen.[59,60] As it was shown by Schmidt[59] the intermolecular repulsive interactions initiate blue shift of about 40 cm^{-1}, which more or less equal for different solvents. It is also known[61] that the S_1 excited-state changes of repulsion between oxygen of carbonyl group and environment for the derivative of 1,8-naphthalimide in diisopropyl ether breaks down the mirror symmetry between absorption and fluorescence spectra for active vibration of 630 cm^{-1}.

The results achieved in fig. 2 for peridinin show a little difference of 35 cm^{-1} between linear regressions when P_n=0 for polar and nonpolar solvents. This minor cross-point difference lies in the limits of experimental error and should be not likely construed to distinction in repulsive effect. Contrary to the structure of molecular oxygen the conjugated system of peridinin is enough shielded from direct contact with solvent molecules and, as did, we can neglect repulsive solvatochromic shift at $S_2 \leftarrow S_0$ transition.

As mentioned above, in Onsager reaction-field treatment[33] of solute-solvent interactions the solute dipole is placed at the center of a spherical cavity. We find that, despite a linear molecular structure of peridinin this simple model with effective cavity radius enables not only to separate out the dispersion, orientation and induced components of universal interactions, but also to find $\mathbf{\Delta\mu}_{eg}$ and $\Delta\alpha_{eg}$. The assigning the molecular structure of peridinin to the idealized C_{2v} point group has enabled to estimate the change of DM between S_0 and S_2 states $\Delta\mu$ of -18.7 D as well as the DM of the S_2 state μ_2 of 12.72 D. Notably, our calculations show that the DM $\mathbf{\mu}_2$ is opposite to that at the ground state $\mathbf{\mu}_g$. It is needed to stress that the DM at the S_2 state $\mathbf{\mu}_2$ does not depend from the nature of solvents at least for the Franck-Condon S_2 state. Some surprising data are presented in fig. 2, because they give an impression that peridinin exhibits two different forms in polar and nonpolar solvents. Therefore one have to keep in mind that, as already noted above, the ν_{00} depends not only on P_n, but on Π_n and P_ε as good see from eqs. (1), (5). The minor intersection difference of 35 cm^{-1} when the standard deviation is of 25 cm^{-1} provides primary evidence that there is only one dominating form of peridinin in the ground state for all solvents or, again, the spectral difference between these forms dose not exceed 85-100 cm^{-1}. This is also to say that H-bonding in protic solvents leaves ν_{00} unaffected or exhibits a little spectral shift.

It is interesting to test if eq. (1) should be applicable for prediction of a thermochromic shift. The spectra of peridinin in MetOH measured at 293 and 190 K are shown in fig. 7. The value $\Delta n/\Delta T = 4 \cdot 10^{-4}$ K^{-1}, n_{293}=1.3270[42] and one can find that ε_{190}=66.24[43]. The eq. (5) predicts the red shift of 220 cm^{-1}

under cooling from 293 to 190 K when the evaluation of 170 cm^{-1} is a mean shift at half-width of spectra $(\delta_1+\delta_2)/2$, in view of intensity redistribution between 0-0 and 0-1 bands. The orientation interactions provide blue shift under cooling while full red solvatochromic shift is accomplished together with induction and dispersion interactions. Despite the low precision of thermochromic shift observations, one can infer that eq. (1) predicts result with tolerable accuracy. Another important feature in the behavior of spectrum under cooling consists in the redistribution of intensity between 0-0 and 0-1 bands with a gain for the latter (fig. 7) that is discussed lower.

8. Anomalous spectral broadening

8.1. *Fluctuations of microenvironment*

For THF, MetOH, ACN, DMSO, EG and Glyc the relative variance Δ^2 is in strong disagreement with eq. (6), which carries out only for simple liquids, for nonpolar Hex, Hept, Benz, CS2 as well as for low polar DEE and 2PrOH. For Glyc the Δ^2 is so high, $1.67 \cdot 10^6$ cm^{-2}, that was not presented in fig. 3. This discrepancy indicates that in addition to the orientation broadening there are some other mechanisms of spectral broadening in called solvents. We emphasize that anomalous broadening occurs for self-associative solvents THF, ACN, MetOH, EG, Glyc as well as for DMSO. Owing to dielectric-loss microwave studies[62-64] the OH···O self-association via H-bonding is the well-known phenomenon for alcohols. It may be safely suggested that in EG and Glyc contained two and three OH functional groups the anomalous broadening is caused by the variety of the branched OH···O-bonded networks which variously interact with peridinin, moreover via H-bonding with carbonyl group. That sets EG and Glyc apart from MetOH and especially from isomeric alcohol 2Prop, which possesses low affinity to H-bonding (fig. 3). High hygroscopic solvent DMSO demonstrates also the high relative variance, perhaps for a similar reason, because it offers ability in H-complexing with water, traces of which inevitably occurs in tested solution. In the theory of solvatochromism, Suppan[65] has deduced that ACN belongs to self-associating liquids due to the forming non-dipolar dimers by pairing of dipoles. It is appropriate to add that such dipole-dipole interactions as the possible reason of cooperative reorientation of the ACN molecules have been considered[66] to interpret the negative entropy of jump reorientation indicated at dielectric loss measurements. Neutron diffraction technique[67] displays a preference for T-like configurations between the THF molecules at room temperature. Thus, we can conclude that the spectral broadening is more sensitive to the local structure of environment of peridinin molecule, whereas the peak position of spectrum is determined by bulk properties of solvent via ε and *n*.

As early exhibited for retinyl compounds[68], additional contribution to spectral broadening of carotenoids may be caused by the existence of conformers differing in their ring-side chain torsional angle. Such inhomogeneous broadening can not be ruled out because jet-cooled spectroscopy[69] of

phenylbutadienyltrimethylcyclohexene gives an indication of conformers with torsional geometry. Nevertheless, one can assume that the effect of conformational disorder due to torsional motion, more or less, is the same for different solvents at the ground state, and there is compensation in variance Δ^2 since it calculated by convolution (7) relative to Hex. Some others components of broadening, e.g. originated from the interaction with local phonons, are also nearly compensated in Δ^2.

Brief mention should be made of red-shifted pump-probe transition spectrum observed in polar solvents by Zigmantas et al.[19] for peridinin and Kosumi et al.[54] for fucoxanthin under excitation in the red region. It was deduced[16,54] that two spectroscopic forms, blue and red, exist in the polar environment. The H-bonding via carbonyl group is assumed[19] to be the origin of the red form in protic solvents. We have used the theory of nonradiative transitions based on the bands-of-energy model of electronic levels[46] to interpret the known data[17,20,21] on the medium polarity effect on the $S_1(A_g^-)$ state lifetime of the apocarotenals[70] and peridinin[71]. We hold to the idea that the internal electric field from solvent environment heavily perturbs the molecules of pigments and changes their structure at $S_1(A_g^-)$ excited state after $S_2 \rightarrow S_1$ relaxation. In consequence of this the pigments possess the excited-state conformers. To take an example, the peridinin exists at $S_1(A_g^-)$ excited state as conformers **I** and **II** with very high DM of 40.7 and 42.8 D respectively.[71] Nevertheless it is unjustified to link these conformers with steady-state absorption, because at the ground $S_0(A_g^-)$ state there is only one actual type of peridinin with strong orientation broadening due to the fluctuations of internal electric field in solution **R**. When pump-probe measurements are carried out the change of excitation energy selects the individual absorber under $S_2 \leftarrow S_0$ transition (well-known in the luminescence[45,51,52] the red-edge effect) and thereby controls the internal electric field at $S_1(A_g^-)$ excited state (see also fig. 8). In the case of peridinin the internal electric field generates two types of excited-state conformers, **I** and **II,** but they are not generated for individual absorbers when **R** is low or equals zero. For this reason either of the two conformers dominates in the solvents of different polarity and practically vanishes in nonpolar solvents. The nature of such conformers is discussed in Refs. [70, 71].

8.2. *Shape variations of individual spectrum* $\kappa_0(\nu,\omega_0)$

Under cooling a characteristic behavior of spectrum for MetOH consists in the strong transformation which involves the increase of intensity at 0-1 band and the decrease of that for 0-0 band (fig. 7). As indicated above, in polar solvents in contrast to nonpolar ones the maximum of absorption spectrum belongs to 0-0 transition. For polar solvents the convolution (7) shows also that the calculated spectrum has lower intensity of the 0-0 band than that from experiment (fig. 4). To understand these observations,

one considers more fully the behavior of spectrum $\kappa_0(\nu,\omega_0)$ of individual peridinin molecule affected the internal electric field.

Shima et al.[13] pointed out that all-trans conformer is preferentially populated in high-dielectric polar solvents such as CS2 and MetOH. We support this evaluation, because the polar molecule of peridinin produces strong Onsager reaction field[32,46]

$$\mathbf{R}_g = 2a_O^{-3}P_\varepsilon\boldsymbol{\mu}_g, \qquad (10)$$

of $8\cdot10^7$ and $20.5\cdot10^7$ V/m for nonpolar Hex and polar MetOH respectively (a_O=9.4 Å^3, μ_g=5.97 D). We believe that all-trans conformer dominates in any solvents, because a reaction field stretches the solute molecule in line with its ground-state DM $\boldsymbol{\mu}_g$ nearly oriented along polyene chain ($\cos\theta$=0.88[17]). Hence it follows also that the shape of individual spectrum $\kappa_0(\nu,\omega_0)$ depends on ω_0 due to a different stretching of polyene chain at the ground S_0 state under the action of fluctuated internal electric field **R**. Because the DM at S_2 state $\boldsymbol{\mu}_2$ has the opposite direction to that at S_0 state $\boldsymbol{\mu}_g$, the stretching gives way to compressing at S_2 state under the $S_2\leftarrow S_0$ transition. Some details of this interpretation are illustrated by the energy level diagrams in fig. 8. The changing from stretching to compressing (or vice versa) provokes the changes of Franck-Condon factor for the different individual absorbers (inset in fig. 8). The concrete numerical example of the change in the pigment length following excitation in S_1 state is described by Enriquez et al.[72], but the solvent can enhance or depress this effect versus the orientation of DM at the excited state.

According to the bands-of-energy model of electronic levels[46] and as shown in fig. 8 the fluctuations of **R** provoke the variation of electronic energy and result in the continuum formation of orientation sublevels at the ground S_0 and excited S_2 states (sparse and equidistant horizontal thick lines). The R_μ denoted the projections of chance internal electric field **R** on the DMs $\boldsymbol{\mu}_g$ and $\boldsymbol{\mu}_e$. The reaction field of medium R_g is mean determined by eq. (10). The orientation sublevels are placed lower or higher relative to the electronic level of pigment molecule unaffected by internal electric field, R_μ=0. The equilibrium sublevel denoted as R_g is placed into the lower part of S_0 continuum. In this region R_μ>0, and the internal electric field induces the stretching of solute molecule; and vise versa, the compressing is observed for the higher part of S_0 continuum. When the direction of peridinin DM is rotated to 180° under the $S_2\leftarrow S_0$ transitions (vertical lines), the stretching of polyene chain at the S_0 state changes to its compressing at the S_2 state, because the projection of electric field R_μ changes sing in strong accordance with Frank-Condon principle. The inset shows the parabolic potential energy diagrams and the changes of generalized coordinate Δq for 1350 cm^{-1} vibration mode via intrinsic repulsion. Thus, the internal electric field leads to a decrease of Huang-Rhys factor in going from blue to red absorbers. The relative intensities of 0-0, 0-1 and other vibration bands are shown by bold vertical lines. Under cooling as well as for more polar solvents the level R_g is lowering[46] and the shape of

spectrum is changed towards the blue absorbers. Nevertheless, the full solvatochromic shift is red because of the induction and strong dispersion interactions (Table 1).

As may be inferred, eqs. (6) and (7), the redistribution of intensity between 0-0 and 0-1 in absorption spectrum depends from solvent polarity P_ε and temperature T. Consequently, the 0-1 band dominates in spectrum for nonpolar solvents (fig.4) and in cooled MeOH (inset in fig. 7).

Overall, we deduce that the anomalous spectral broadening in polar solvents has originates mainly in the fluctuations of microstructure and in the rearrangements into the solvation shell of peridinin due to specific interactions between solvent molecules. The fluctuations of the local structure in turn change the universal and short-range solute-solvent interactions. Anomaly is enhanced by the shape variation of individual spectrum $\kappa_0(\nu,\omega_0)$ which is caused by fluctuation of internal electric field **R**.

Conclusion

There is good reason to think that the full solvatochromic calculations combined with convolution estimations of orientation broadening may be effective tool in study of electrostatic properties not only peridinin, but other carotenoids as well. The large change of DM $|\mathbf{\Delta\mu}|$ of 18.7 D under $S_2 \leftarrow S_0$ transition is corroborated by Stark spectroscopy research from Grondelle group.[25] The negative change of $\Delta\mu$ relative to DM at the S_0 state have been demonstrated by the Birge group[27] via SAC-CI methods, however before our calculation the opposite orientation of $\mathbf{\mu}_2$ is conclusively not argued. We evaluated that the gas-phase 0-0 electronic energy of the $S_2 \leftarrow S_0$ transition $\nu_{0\text{-}0}$=22910 (±80) cm^{-1} (2.84 eV). The error ±80 cm^{-1} causes both the mistakes with regression and an uncertainty in repulsive and H-bonding effects. The obtained $\nu_{0\text{-}0}$ provides the change of polarizability between S_0 and S_2 states $\Delta\alpha_{eg}$=376 $Å^3$ by eq. (9) in accordance with new formula for the dispersion solvatochromic shift[40]. In comparison with $\nu_{0\text{-}0}$ of 2.84 eV the MNDO-PSDCI calculations[13] predict the energies of 1.96, 2.39 and 2.80 eV for the A_g^-, B_u^+ and B_u^--like excited states respectively, in the case of all-trans conformer. It is worth noting that the resemblance with 2.80 eV for optically forbidden B_u^--like state is accidental. It is likely that the EOM-CCSD methods are more accurate.[27] One would expect a further efforts will be required to perfect the quantum-mechanical calculations both transition energies and excited-state electrostatic properties. Of special interest are the angles between $\mathbf{\mu}_g$ and excited-state DMs. Based on the large change in DM we support opinion[25] that S_2 state (B_u^+-like) possesses CT character.

Acknowledgments

Author is grateful to Professors T. Polivka and V. Sundström for kindly offering of the experimental data and discussions. I thank also Olga Koverko, my former diploma student, for software to convolution evaluations.

Key words:

solvatochromic shift
excited-state dipole moment
excited-state polarizability
spectral broadening
peridinin

Figure 1.

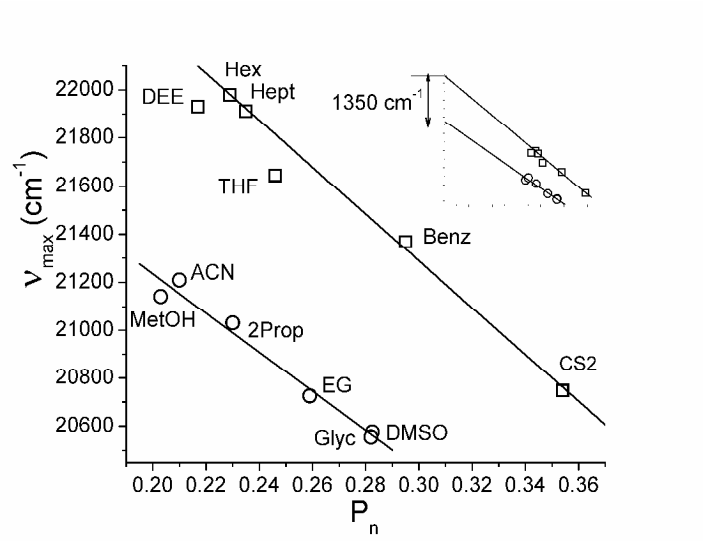

Figure 1. Experimental absorption maximum ν_{max} as a function of the solvent polarizability P_n. The linear regressions obtained for Hex, Hept, Benz, CS2 as well as for MetOH, ACN, 2Prop, EG, DMSO, Glyc are ν_{max}=24213.6-9749.8P_n and ν_{exp}=22863.9-8145.7P_n respectively. The points for DEE and THF do not take in attention under regression (see details in text). The inset shows a cross-point difference of 1350 cm^{-1} at P_n=0.

Figure 2.

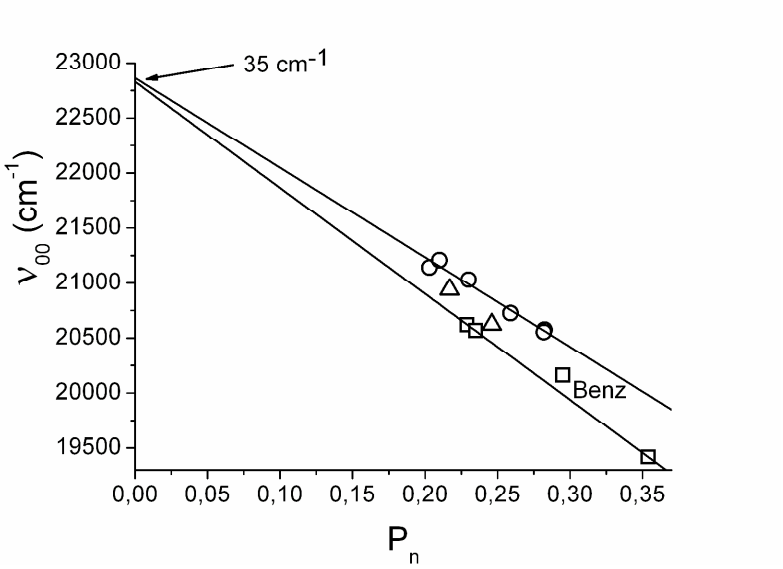

Figure 2. Plots of 0-0 band maximum ν_{00} versus P_n. The linear regression ν_{00}=22828.8-9636.1P_n is presented only for Hex, Hept, and CS2 (lower solid line). The points for DEE, THF (triangles) and Benz do not take in attention under fitting. Other linear regression, ν_{00}=22863.9-8145.7P_n, for MetOH, ACN, 2Prop, EG, DMSO, Glyc coincides with that shown in fig. 1. Cross-point difference is of 35 cm^{-1}.

Figure 3.

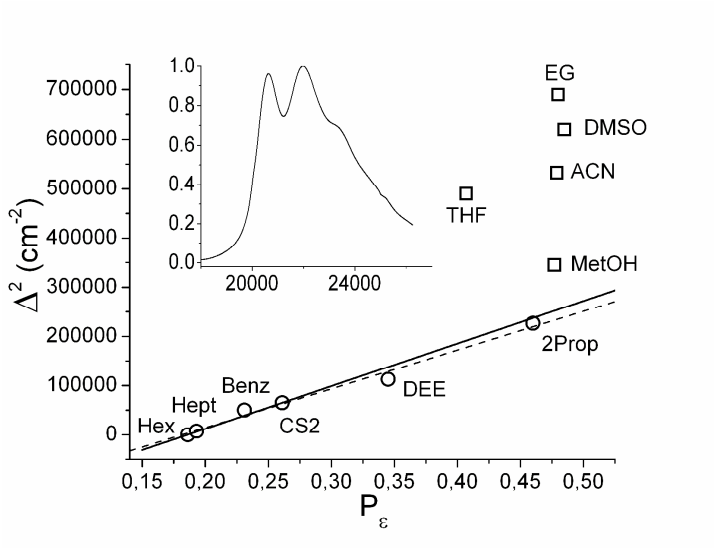

Figure 3. Dependence of the relative variance Δ^2 on the solvent polarity P_ε, and solid line with slope of 866160 cm^{-2} connecting two points, namely Hex (zero) and CS2 (64962 cm^{-2}). The dash line shows the linear regression for Hex, Hept, Benz, CS2, DEE and 2Prop with slope of 789110 cm^{-2}. The inset displays the spectrum of peridinin in Hex, which was used as a reference spectrum $\kappa_0(\nu,\omega)$ in eq. (7) to evaluate Δ^2.

Figure 4.

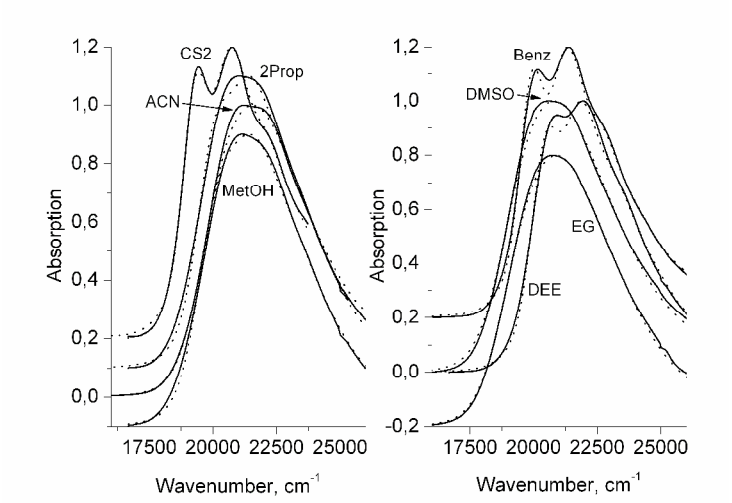

Figure 4. Examples of comparison of the normalized experimental $\kappa_{exp}(\nu)$ and calculated $\kappa(\nu)$ spectra (solid and dots respectively) for peridinin in CS2, 2Prop, ACN, MetOH (left panel), Benz, DMSO, DEE, EG (right panel). In order to make the best use spectra are displaced in ordinates.

Figure 5.

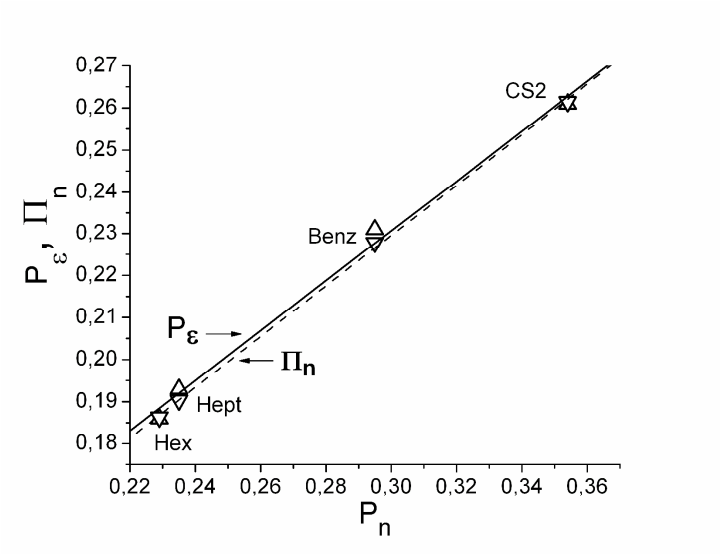

Figure 5. The linear plots P_ε versus P_n as well as Π_n versus P_n for nonpolar solvents, Hex, Hept, Benz, CS2.

Figure 6.

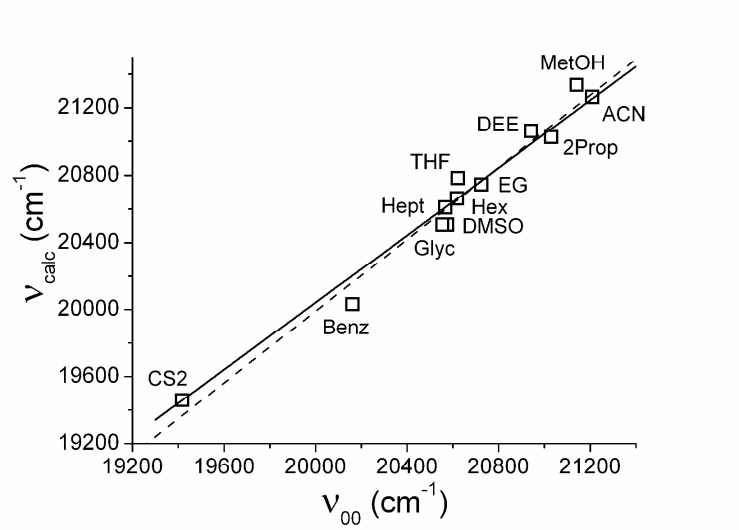

Figure 6. Comparison of calculated 0-0 transitions with experimental maximum ν_{00}, in accordance with eq. (5) ν_{calc}=22909+1358P_ε-2126Π_n-9179P_n. The solid line with slope of 1.0021 shows the liner regression for base solvent Hex, Hept and CS2, r=1. The dash line with slope of 1.0708 displays the liner regression for all points, r=0.9862.

Figure 7.

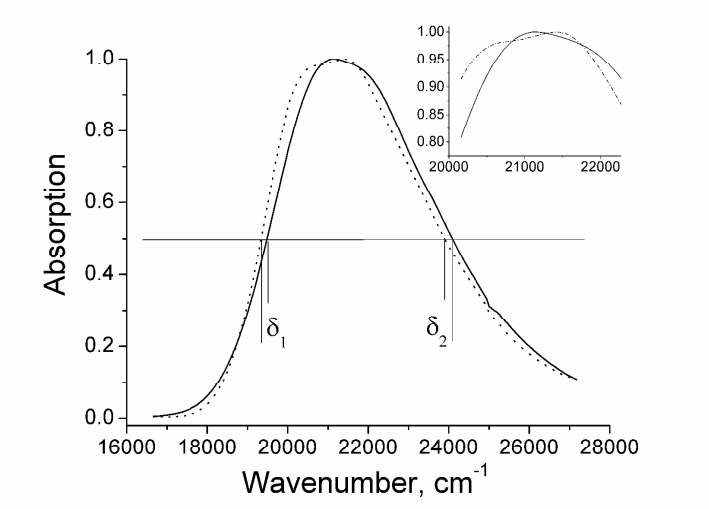

Figure 7. Changes in absorption spectrum of peridinin in MeOH under cooling. Solid and dot lines show spectra measured at 293 and 190 K respectively. Inset illustrates the enlargement around the maximum.

Figure 8.

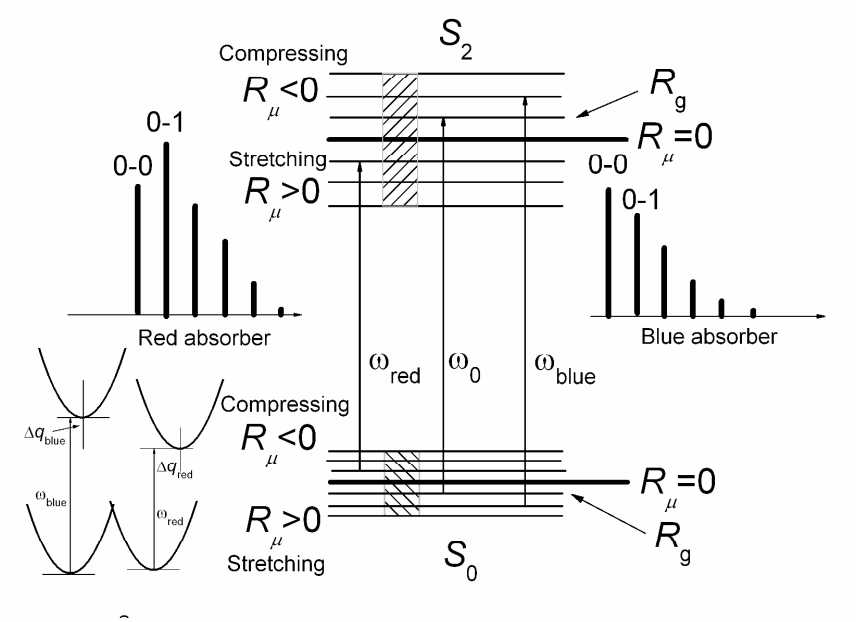

Figure 8. Effect of internal electric field **R** on the vibrinic absorption spectrum for blue and red individual absorbers in light of bands-of-energy model of electronic levels[46] (see details in text).

References and notes

[1] H. A. Frank and R. J. Cogdell, Carotenoids in photosynthesis, *Photochem. Photobiol.*, 1996, 63, 257-264.

[2] R. J. Cogdell and H. A. Frank, How carotenoids function in photosynthetic bacteria, *Biochim. Biophys. Acta*, 1987, **895**, 63–79.

[3] M. Mimuro, U. Nagashima, S. Takaichi, Y. Nishimura, I. Yamazaki and T. Katoh, Molecular structure and optical properties of carotenoids for the in vivo energy transfer function in the algal photosynthetic pigment system, *Biochim. Biophys. Acta*, 1992, **1098**, 271–274.

[4] A. Young and H. A. Frank, Energy transfer reactions involving carotenoids: quenching of chlorophyll fluorescence, *Photochem. Photobiol. B: Biology*, 1996, **36**, 3–15.

[5] R. Edge, D. J. McGarvey and T.G. Truscott, The carotenoids as anti-oxidants – a review, *J. Photochem. Photobiol. B: Biology*, 1997, **41**, 189–200.

[6] T. Ritz, A. Damjanovic, K. Schulten, J.-P. Zhang and Y. Koyama, Efficient light harvesting through carotenoids, *Photosynth. Res.*, 2000, **66**, 125–144.

[7] T. Polivka and V. Sundström, Ultrafast dynamics of carotenoid excited states – from solution to natural and artificial systems, *Chem. Rev.*, 2004, **104**, 2021–2071.

[8] R. L. Christensen, The electronic states of carotenoids, in *Photochemistry of Carotenoids* (Eds: A. J. Young, G. Britton, R. J. Cogdell), Kluwer Academic Publisher, Dordrecht, 1999**,** pp. 137–157.

[9] R. L. Christensen, M. Goyette, L. Gallagher, J. Duncan, B. DeCoster, J. Lugtenburg and I. van der Hoef, S_1 and S_2 states of apo- and diapocarotenes, *J. Phys. Chem. A*, 1999, **103**, 2399–2407.

[10] P. Tavan and K. Shulten, Electronic excitations in finite and infinite polyenes, *Phys. Rev. B,* 1987, **36**, 4337–4358.

[11] T. Sashima,; Nagae, M. Kuki and Y. Koyama, A new singlet-excited state of all-*trans*-spheroidene as detected by resonance-Raman excitation profiles, *Chem. Phys. Lett.*, 1999, **299**, 187–194.

[12] T. Sashima, Y. Koyama, T. Yamada and H. Hashimoto, The $1B_u^+$, $1B_u^-$, and $2A_g^-$ energies of crystalline lycopene, β-carotene, and mini-9-β-carotene as determined by resonance-Raman excitation profiles: Dependence of the $1B_u^-$ state energy on the conjugation length, *J. Phys. Chem. B*, 2000, 104, 5011–5019.

[13] S. Shima, R. P. Ilagan, N. Gillespie, B. J. Sommer, R. G. Hiller, F.P. Sharples, H. A. Frank and R. R. Birge, Two-photon and fluorescence spectroscopy and the effect of environment on the photochemical properties of peridinin in solution and in the peridinin-chlorophyll-protein from *Amphidinium carterae*, *J. Phys. Chem. A*, 2003, **107**, 8052–8066.

[14] E. Hofmann, P. Wrench, F. Sharples, R. G. Hiller, W. Welte and K. Diederichs, Structural basis of light harvesting by carotenoids: Peridinin-chlorophyll-protein from *Amphidinium carterae*, *Science*, 1996, **272**, 1788–1791.

[15] H. S.Yoon, J. D. Hackett and D. Bhattacharya, A single origin of the peridinin- and fucoxanthin-containing plastids in dinoflagellates through tertiary endosymbiosis, *Proc. Natl. Acad. Sci. U.S.A.*, 2002, **99**, 11724–11729.

[16] J.A. Bautista, R.E. Connors, B.B. Raju, R.G. Hiller, F.P. Sharples, D. Gosztola, M.R. Wasielewski and H.A. Frank, Excited state properties of peridinin: observation of a solvent dependence of the lowest excited singlet state lifetime and spectral behavior unique among carotenoids, *J. Phys. Chem. B*, 1999**,** **103***,* 8751–8758.

[17] H. A. Frank, J. A. Bautista, J. Josue, Z. Pendon, R. G. Hiller, F. P. Sharples, D. Gosztola and M. R. Wasielewski, Effect of the solvent environment on the spectroscopic properties and dynamics of the lowest excited states of carotenoids, *J. Phys. Chem. B*, 2000, **104**, 4569–4577.

[18] D. Zigmantas, T. Polivka, R. G. Hiller, A. Yartsev and V. Sundström, Spectroscopic and dynamic properties of the peridinin lowest singlet excited states, *J. Phys. Chem. A*, 2001, **105,** 10296–10306.

[19] D. Zigmantas, R. G. Hiller, A. Yartsev, V. Sundström and T. Polivka, Dynamics of excited states of the carotenoid peridinin in polar solvents: Dependence on excitation wavelength, viscosity, and temperature, *J. Phys. Chem. B*, 2003, **107,** 5339–5348.

[20] M. Kopczynski, F. Ehlers, T. Lenzer and K. Oum, Evidence for an Intramolecular Charge Transfer State in 12'-apo-β-caroten-12'-al and 8'-apo-β-caroten-8'-al: Influence of Solvent Polarity and Temperature, *J. Phys. Chem. A*, 2007, **111,** 5370–5381.

[21] F. Ehlers, T. Lenzer and K. Oum, Excited-State Dynamics of 12′-Apo-β-caroten-12′-al and 8′-Apo-β-caroten-8′-al in Supercritical CO_2, N_2O, and CF_3H, *J. Phys. Chem. B*, 2008, **112**, 16690–16700.

[22] T. Polivka, S. Kaligotla, P. Chabera and H. A. Frank, An intramolecular charge transfer state of carbonyl carotenoids: implications for excited state dynamics of apo-carotenals and retinal, *Phys. Chem. Chem. Phys*., 2011, **13**, 10787–10796.

[23] M. Fuciman, M. M. Enriquez, S. Kaligotla, D. M. Niedzwiedzki, T. Kajikawa, K. Aoki, S. Katsumura and H. A. Frank, Singlet and Triplet State Spectra and Dynamics of Structurally Modified Peridinins, *J. Phys. Chem. B***,** 2011, **115**, 4436–4445.

[24] H. Vaswani, C. Hsu, M. Head-Gordon and G. R. Fleming, Quantum chemical evidence for an intramolecular charge-transfer state in the carotenoid peridinin of peridinin-chlorophyll-protein, *J. Phys. Chem. B***,** 2003, **107**, 7940–7946.

[25] L. Premvardhan, E. Papagiannakis, R. G. Hiller, and R. van Grondelle, The charge-transfer character of the $S_0 \rightarrow S_2$ transition in the carotenoid peridinin is revealed by Stark spectroscopy, *J. Phys. Chem. B*, 2005, **109**, 15589–15597.

[26] L. Premvardhan, D. J. Sandberg, H. Fey, R. Birge, C. Büchel and R. van Grondelle, The charge-transfer properties of the S_2 state of fucoxanthin in solution and in fucoxanthin chlorophyll-a/c_2 protein (FCP) based on Stark spectroscopy and molecular-orbital theory, *J. Phys. Chem. B*, 2008, **112**, 11838–11853.

[27] N. L. Wagner, J. A. Greco, M. M. Enriquez, H. A. Frank and R. R. Birge, The nature of the intramolecular charge transfer state in peridinin, *Biophys. J.*, 2013, **104**, 1314–1325.

[28] V. S. Pavlovich, Role of the medium in radiationless conversion of the energy of the excited S_1 state in equilibrium systems with intramolecular charge transfer, *J. Appl. Spectrosc*., 2004, **71**, 60–67.

[29] V. S. Pavlovich, Solvent polarity effect on excited-state lifetime of carotenoids and some dyes, *Biopolymers*, 2006, **82**, 435–441.

[30] E. Papagiannakis, D. S. Larsen, I. H. M. van Stokkum, M. Vengris, R. G. Hiller and R. van Grondelle, *Biochemistry*, Resolving the excited state equilibrium of peridinin in solution, 2004, **43**, 15303–15309.

[31] E. Papagiannakis, M. Vengris, D. S. Larsen, I. H. M. van Stokkum, R. G. Hiller and R. van Grondelle, Use of ultrafast dispersed pump-dump-probe and pump-repump-probe spectroscopies to explore the light-induced dynamics of peridinin in solution, *J. Phys. Chem. B*, 2006, **110**, 512–521.

[32] V. S. Pavlovich, Polarity of the medium and quenching of fluorescence of carotenoids and phthalimides, *J. Appl. Spectrosc*., 2004, **71**, 359–365.

[33] L. Onsager, Electric moment of molecules in liquids, *J. Am. Chem. Soc.*, 1936, **58**, 1486–1493.

[34] Y. Ooshika, Absorption spectra of dyes in solution, *J. Phys. Soc. Jap.*, 1954**, 9***,* 594–602.

[35] E. Lippert, Dipolmoment und Elektronenstruktur von angeregten Molekülen, *Z. Naturforsch. A*, 1955**, 10**, 541–545.

[36] N. Mataga, Y. Kaifu and M. Koizumi, The solvent effect on fluorescence spectrum, change of solute-solvent interaction during the lifetime of excited solute molecule, *Bull. Chem. Soc. Jap.*, 1955**, 28**, 690–691.

[37] N. Mataga, Y. Kaifu and M. Koizumi, Solvent effects upon fluorescence spectra and the dipole moments of excited molecules, *Bull. Chem. Soc. Jap.*, 1956**, 29**, 465–470.

[38] E. Lippert, Spektroskopische Bestimmung des Dipolmomentes aromatischer Verbindungen im ersten angeregten Singulettzustand, *Ber. Bunsenges. Phys. Chem.*, 1957, **61**, 962–975.

[39] E.G. McRae, Theory of solvent effects on molecular electronic spectra. Frequency shifts, *J. Phys. Chem.*, 1957, **61**, 562–572.

[40] E. Lippert, W. Lüder, F. Moll, W. Nägele, H. Boos, H. Prigge, I. Seibold-Blankenstein, Umwandlung von Elektronenanregungsenergie, *Angew. Chem.*, 1961, **73**, 695–706.

[41] V. S. Pavlovich, Dispersion interactions, electronic absorption spectra of anthracenes in polar glassy media at 77–300 K, and the change in polarizability upon excitation, *J. Appl. Spectrosc.*, 2007, **74**, 180–187.

[42] *Chemist's Handbook*, Vol. 1, GNTI Khim. Lit., Leningrad/Moscow, 1962 [in Russian].

[43] J. J. Ahadov, *Dielectric properties of pure liquids*, Standarty, Moscow, 1972 [in Russian].

[44] *Aldrich*, USA, Aldrich Chemical Company, Inc., 1992.

[45] A. P. Demchenko, The red-edge effects: 30 years of exploration, *Luminescence*, 2002, **17**, 19–42.

[46] V. S. Pavlovich, Solvatochromism and nonradiative decay of intramolecular charge-transfer excited states: Bands-of-Energy model, thermodynamics, and self-organization, *Chem. Phys. Chem.*, 2012, **13**, 4081–4093.

[47] V.S. Pavlovich, Fluctuations of local electric field in polar media and variance of electron transition frequency-distribution of polar impurity molecules, *Dokl. Akad. Nauk BSSR* (Minsk), 1987, **31**, 412–415.

[48] V.S. Pavlovich, Effect of orientation solvation on the vibronic spectra of polar molecules in solution, *Weszi Akad. Nauk BSSR, Ser. Fiz.–Mat. Nauk* (Minsk), 1987, No. 6, 55–61.

[49] V.S. Pavlovich, Histons: New Quasi-particles and Time-Resolved Fluorescence Shift of Polar Disordered Media, *J. Fluoresc.*, 1997, **7**, 321–329.

[50] R.A. Marcus, On the theory of shifts and broadening of electronic spectra of polar solutes in polar media, *J. Chem. Phys.*, 1965, .**43**, 1261–1274

[51] V.S. Pavlovich and L. G. Pikulik, Dependence of the fluorescence spectra of solutions of complex molecules on the exciting light, *J. Appl. Spectrosc.*, 1972, **16**, 753–757.

[52] V.S. Pavlovich, The dependence of the excitation spectra of solutions of dipole molecules on the recording wavelength, *J. Appl. Spectrosc.*, 1976, **25**, 1141–1147.

[53] H. Cramér, *Mathematical methods of statistics,* Princeton University Press, Princeton, 1991.

[54] D. Kosumi, T. Kusumoto, R. Fujii, M. Sugisaki, Y. Iinuma, N. Oka, Y.Takaesu, T. Taira, M. Iha, H. A. Frank and H. Hashimoto, Ultrafast excited state dynamics of fucoxanthin: excitation energy dependent intramolecular charge transfer dynamics, *Phys. Chem. Chem. Phys.*, 2011, **13**, 10762–10770.

[55] S. Volker, Hole-burning spectroscopy, *Annu. Rev. Phys. Chem.,* 1989, **40**, 499–530.

[56] S. Krawczyk and D. Olszowka, Spectral broadening and its effect in Stark spectra of carotenoids, *Chem. Phys*., 2001, *265*, 335–347.

[57] R. J. W. Le Fevre, Molecular refractivity and polarizability, *Adv. Phys. Org. Chem.*, 1965, **3**, 1–90.

[58] N. G. Bakshiev, Spectroscopy of Intermolecular Interactions, Nauka, Leningrad, 1972 [in Russian].

[59] R. Schmidt, Solvent Shift of the $^1\Delta_g \rightarrow {}^3\Sigma_g^-$ Phosphorescence of O_2, *J. Phys. Chem. B*, 1996, **100**, 8049–8052.

[60] V. S. Pavlovich, Solvatochromic shift of the 0-0 phosphorescence band and change of polarizability in the $a^1\Delta_g \rightarrow X^3\Sigma_g^-$ transition in the oxygen molecule, *J. Appl. Spectrosc*., 2007, **74**, 501–507.

[61] V. S. Pavlovich, A.P. Lugousky, D.I. Sagaydak and A.P.Stupak, Photophysical properties of powder and solutions of *N*-(*p*-methoxyphenyl)-4-octylamino-1,8-naphthalimide, *J. Appl. Spectrosc*., 2013, **80**, 524–529.

[62] F. X. Hassion and R. H. Cole, Dielectric properties of liquid ethanol and 2-propanol, *J. Chem. Phys*., 1955, **23**, 1756–1761.

[63] W. Dannhauser and R. H. Cole, Dielectric properties of liquid butyl alcohols, *J. Chem. Phys*., 1955, **23**, 1762–1766.

[64] D. J. Denney and R. H. Cole, Dielectric Properties of Methanol and Methanol-1-Propanol Solutions, *J. Chem. Phys*., 1955, ***23***, 1767–1772.

[65] P. Suppan, Solvatochromic shifts: the influence of the medium on the energy of electronic states, *J. Photochem. Photobiol. A: Chemistry*, 1990, **50**, 293–330.

[66] Krishnaji, A. Mansingh, Dielectric Relaxation in Alkylcyanides, *J. Chem. Phys*., 1964, **41**, 827–831.

[67] D. T. Bowron, J. L. Finney and A. K. Soper, The structure of liquid tetrahydrofuran, *J. Am. Chem. Soc*., 2006, **128**, 5119–5126.

[68] B. E. Kohler, Visual chromophore electronic structure, *Biophys. Struct. Mechanism*, 1977, **3**, 101–106.

[69] J. P. Finley and J. R. Cable, Electronic spectroscopy of jet-cooled phenylbutadienyltrimethylcyclohexene, *Chem. Phys. Lett*., 1994, **228**, 9–14.

[70] V. S. Pavlovich, Nonradiative transitions in the media of different polarity and their simulations for 12'-apo-β-caroten-12'-al and 8'-apo-β-caroten-8'-al, *J. Appl. Spectrosc*., 2014, **81**, xxx–yyy.

[71] V. S. Pavlovich, *Dokl. Akad. Nauk Belarusi* (Minsk), Decay of S_1 state of peridinin in the media of different polarity and conformers, 2014**, 58**, xxx–yyy.

[72] M. M. Enriquez, S. Hananoki, S. Hasegawa, T. Kajikawa, S. Katsumura, N. L. Wagner, R. R. Birge and H. A. Frank, Effect of molecular symmetry on the spectra and dynamics of the intramolecular charge transfer (ICT) state of peridinin, *J. Phys. Chem. B.*, 2012, **116**, 10748–10756.

Table 1. Experimental absorption maximum ν_{max} and peak position of 0-0 transition ν_{00}, peak position of 0-0 transition calculated by eq. (5) ν_{calc}, bulk solvent properties P_n, P_ε and Π_n, full calculated solvatochromic shift $\Delta\nu_{calc}$ and its dispersion $\Delta\nu_{dis}$, orientation $\Delta\nu_{or}$ and induction $\Delta\nu_{ind}$ components for peridinin in solutions at 293 K. All values ν and $\Delta\nu$ (cm^{-1}) are rounded to 1 cm^{-1}.

Solvent	ν_{max}	ν_{00}	ν_{calc}	P_n	P_ε	Π_n	$\Delta\nu_{calc}$	$\Delta\nu_{dis}$	$\Delta\nu_{or}$	$\Delta\nu_{ind}$
MetOH	21142	21142	21335	0.203	0.477	0.169	-1574	-1863	648	-359
MetOH, 190 K	21413	~20700	21117	0.225	0.489	0.184	-1792	-2065	664	-391
ACN	21209	21209	21263	0.210	0.479	0.1735	-1647	-1928	650	-369
DEE	21930	20942	21061	0.217	0.385	0.178	-1848	-1992	523	-379
Hex	21978	20619	20663	0.229	0.186	0.186	-2245	-2102	253	-396
2Prop	21031	21031	21025	0.230	0.460	0.187	-1881	-2111	627	-397
Hept	21911	20568	20609	0.235	0.193	0.190	-2299	-2157	262	-404
THF	21645	20623	20784	0.246	0.407	0.197	-2125	-2258	553	-420
EG	20725	20725	20746	0.259	0.48	0.206	-2162	-2377	652	-437
Glyc	20555	20555	20507	0.282	0.482	0.220	-2402	-2588	654	-468
DMSO	20576	20576	20506	0.2825	0.485	0.220	-2402	-2593	659	-468
Benz	21368	20161	20031	0.295	0.231	0.228	-2878	-2708	314	-484
CS2	20747	19418	19458	0.354	0.261	0.2615	-3451	-3249	354	-556

Table 2. Relative variance Δ^2 obtained by eq. (7) at 293 K, the variance $D^2_{solv} = \Delta^2 + D^2_{Hex}$, the variance D^2 calculated by eq. (6), and FWHM $\Gamma = 2\sqrt{2\ln 2}D$ for peridinin in solvents of different polarity P_ε.

Solvent	P_ε	Δ^2, cm^{-2}	D^2_{solv}, cm^{-2}	D^2, cm^{-2}	Γ, cm^{-1}
Hex	0.186	0	161106	161132	945
Hept	0.193	7184	168290	167196	963
Benz	0.231	50202	211308	200115	1053
CS2	0.261	64962	226068	226104	1120
DEE	0.385	112382	273488	333525	1360
THF	0.407	489923	651029	352582	1398
2Prop	0.460	226283	387389	398498	1487
MetOH	0.477	344848	505954	413225	1514
MetOH, 190 K	0.489			274562	1234
ACN	0.479	532592	693698	414957	1517
EG	0.480	689446	850552	415824	1518
Glyc	0.482	$1.67 \cdot 10^6$	1831110	417556	1522
DMSO	0.485	619606	780712	420155	1526